GROWTH IN SYSTEMS WITH QUENCHED DISORDER

(in *Growth Patterns in Physical Sciences and Biology*, Edited by J. M. Garcia-Ruiz, L. Sander and P. Meakin (Plenum, New York, 1993) pp. 65-75.)

Mark O. Robbins, Marek Cieplak, Hong Ji, Belita Koiller and Nicos Martys

Department of Physics and Astronomy
The Johns Hopkins University
Baltimore, MD 21218

INTRODUCTION

In this paper we consider the effect of quenched disorder on growth. Two specific examples are considered to illustrate the general nature of the changes induced by disorder: magnetic domain growth[1–3] and immiscible fluid invasion.[4–8] In each case there are two domains which have different spin orientations or fluid composition. An applied force, magnetic field or pressure, favors growth of one domain.

Several universal features are found in all systems studied.[1–8] The first is that disorder pins the interface between domains. The interface can only advance continuously when a critical force, f_c, is exceeded. Three types of morphology are found for the marginally stable interfaces at f_c: faceted, self-affine and self-similar. Faceted interfaces are found in the limit of weak disorder where lattice anisotropy becomes important. When the degree of disorder is large, the interface is a self-similar fractal characteristic of percolation.[9] Self-affine interfaces are found at intermediated degrees of disorder in some models. The transitions between these growth morphologies are critical phenomena characterized by diverging coherence lengths.

The onset of interface motion is also a critical phenomena in the self-similar and self-affine regimes. Increasing the force towards f_c produces larger and larger incremental advances of the interface. Their mean size diverges at f_c and they follow a power law distribution. The exponents describing these and other quantities can be related through scaling laws.[6] Only the fractal dimensions and a single additional exponent are needed to determine all other exponents.

We begin by describing the growth rules used in our studies. Then results are presented with an emphasis on universal trends. These are primarily illustrated for the magnetic system which is conceptually simpler. The final section of the paper presents a summary and conclusions.

GROWTH MODELS

The Hamiltonian and rules for domain wall motion are described in detail in reference.[1] Ising spins $s_i = \pm 1$ are placed on each site i of a 2 or 3D array. Their Hamiltonian, in units of the exchange coupling, is

$$\mathcal{H} = -\sum_{<i,j>} s_i s_j - \sum_i (h_i + H) s_i \ . \tag{1}$$

The first term is a nearest-neighbor spin-spin exchange interaction. The second term describes the interaction of each spin with the sum of the local random field h_i and a uniform external magnetic field H. Values of h_i are generated randomly following some probability distribution function $P(h)$. Several forms for P have been studied,[2] but the behavior is mainly dominated by the bounds of $P(h)$. In this paper we restrict our attention to uniform distributions: $P(h) = (2\Delta)^{-1}$ for $|h| < \Delta$. The value of Δ characterizes the degree of disorder. It represents the ratio of the size of the random fields to the exchange coupling which favors aligned spin states.

Spins at the bottom edge of the simulation cell are originally "flipped" ($s = +1$), while all other spins are "unflipped" ($s = -1$). To mimic the process of fluid invasion, growth occurs at zero temperature and *only spins at the interface are allowed to flip.* An interface spin is flipped when this lowers the total energy of the system. If there is more than one unstable spin on the interface, the most unstable spin is flipped first. Each spin-flip alters the exchange interaction on neighboring interface spins or adds new spins to the interface. Thus a single spin-flip may produce a chain reaction. Once a spin is flipped, it does not return to the unflipped state.

The overall advance of the interface is controlled by the value of the external field H, which is varied quasistatically. It is initially taken to be the smallest value, H_0, that causes a single spin on the interface to flip. This single change in the spin array may cause neighboring spins to flip, which may induce subsequent spin flips. The external field value is kept equal to H_0 until a stable interface is attained. Then H is increased so that a single spin flip occurs on the new interface, and the procedure is repeated until the interface reaches the top of the system. The value of H required for the pattern of flipped spins to span the system rapidly approaches a limiting critical field H_c as the number of spins along an edge of the cell, L, increases.

It is convenient at this point to identify quantities which describe the importance of the local environment in producing spin-flips.[2] These will be useful in the discussion of the critical transitions below. Whether a spin s_i at the interface flips depends on the value of the external field H, the value of the local random field h_i, and the state of the z nearest-neighbor spins. The fraction of spins with n flipped neighbors which will flip at the critical field is

$$f_n = \int_{-\infty}^{H_c} P(z - 2n - H) dH = (H_c - z + 2n + \Delta)/2\Delta \quad , \tag{2}$$

where the last equality holds only for uniform distributions and for $|H_c - z + 2n| < \Delta$.

Fluid invasion has been studied in two different types of model 2D porous media.[4–8] The first consists of ducts of random width placed along the bonds of a square network.[8] Such models have been studied in experiments by several groups.[10–13] The second class of porous media was constructed[4–6] by placing disks of random radii on the sites of a square or hexagonal lattice of lattice constant a. This model is closer to a cross-section through a glass bead pack – another common model system.[14–19]

The effective degree of disorder in these porous media depends on two factors. The first factor is the degree of geometrical disorder in the pore space. In the case of duct

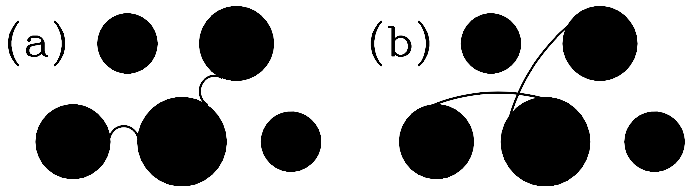

Figure 1: Arcs connecting successive beads along the interface for (a) $\theta = 180°$ and (b) $\theta = 30°$. The invading fluid is advancing from below, and the bond angle between three successive disks along the interface is $\alpha = 120°$.

networks this is characterized by $R = d_{max}/d_{min}$, the ratio between the maximum and minimum duct widths. The ratio between the maximum and minimum widths of the throats between disks provides a similar measure in the disk model. The second important factor is the relative wetting tendency of the invading fluid. This can be quantified by the contact angle θ (measured through the invading fluid) at which the fluid interface intersects the solid.

Figure 1 illustrates why θ controls the effective interaction between neighboring pores. The invading fluid is driven forward by an external pressure P. In quasi-static invasion this pressure drop appears everywhere along the interface. In 2D, the interface consists of circular arcs with curvature P/γ, where γ is the surface tension and the boundary of the invading fluid is convex for positive pressures. These arcs must also intersect the disks or duct walls at θ.

When the invading fluid is non-wetting, the narrow ducts or throats between disks are the hardest to penetrate because the required pressure is largest (Fig. 1(a)). Arcs are confined within their respective throats, and neighboring arcs advance independently. The situation is much like that in a magnetic system with no exchange coupling between spins. When the invading fluid is more wetting, arcs are sucked rapidly through the narrow throats and the pore spaces are the hardest regions to pass. Since arcs in neighboring throats share a common pore space, interactions between them are enhanced. In Fig. 1(b) each arc would be stable individually. However, when both are present in the pore they *overlap* and the kink in their combined interface is unstable. The probability of an overlap depends on the bond angle α between successive disks along the interface. In the figure $\alpha = 120°$. If the interface connected three beads in a line ($\alpha = 180°$) the arcs would no longer overlap for this pressure, contact angle, and geometry. Thus overlaps preferentially remove sharp bends in the interface (small α). They act much like an exchange coupling in maintaining a coherent domain. However, in the magnetic case only the number of surroundings spins of each type is important. In the fluid case, the relative position of the throats determines α and thus the condition for stability. Since overlaps become more likely as θ decreases, the effective degree of coupling increases and the relative degree of disorder decreases.

Growth was initiated from a flat interface or central ring. The algorithm is much like that for magnetic domain growth, with pressure P replacing the external field H. The initial value of P was set to P_0, the pressure at which the first segment of the interface became unstable. This segment of the interface was advanced. Any resulting instabilities were advanced in turn until a new stable interface was reached. The value of P was then increased until a segment of this interface became unstable, and the process was repeated. For each θ we identified a critical pressure P_c at which the invading fluid would first span an infinite system.

The major difference between our magnetic and fluid studies is in the treatment of "trapped regions".[11,20] In some cases, advancing a segment causes the interface to

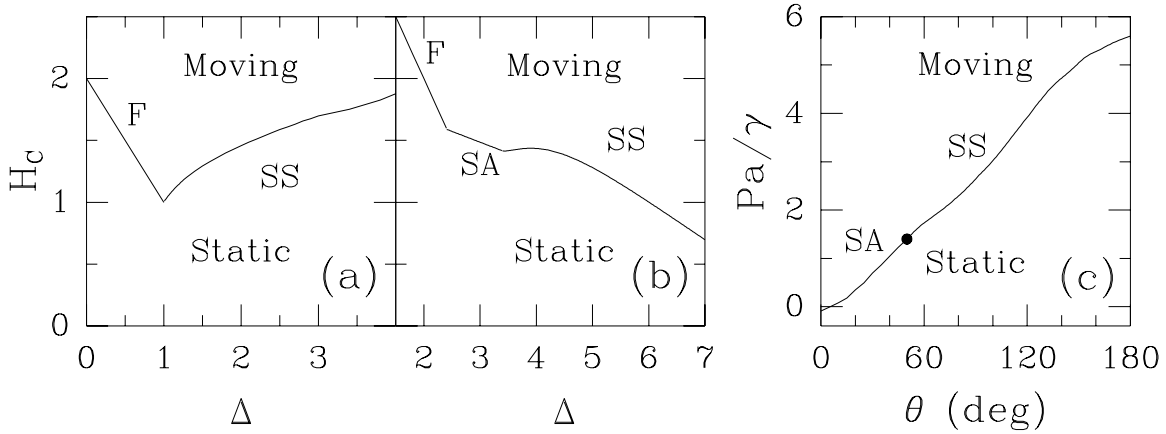

Figure 2: Phase diagrams for magnetic domain growth on the (a) square and (b) cubic lattices, and for fluid invasion of (c) a hexagonal array of disks. A curve in each panel indicates the critical force separating static and moving states of the interface. The large scale structure of the interface at the critical force is indicated by SS for self-similar interfaces, SA for self-affine interfaces and F for faceted interfaces. In (a) there is a direct transition from self-similar to faceted growth. In (b) there is an intermediate self-affine regime. A dot indicates the transition to self-affine growth in (c). The faceted regime is suppressed in this highly disordered system.

completely surround a region of the defending fluid. This trapped region can not shrink further if the fluid is incompressible. We implemented this rule in studies of the random disk model, but not in studies of the duct network or magnetic domain models. Trapping may change the fractal dimension slightly[20] in 2D, but does not change the transitions in growth morphology discussed below.[1–8]

The above growth algorithms are useful for studies of the approach to the critical force from the pinned regime. Different algorithms are needed to study steady-state motion at forces greater than the critical force. Two rules for advancing unstable segments of the interface were used. One was an Eden-like model[21] in which the growth site was chosen randomly from the set of unstable segments. The second was a synchronous update rule where all unstable segments at a given time step were advanced before any subsequent instabilities were considered. These algorithms produce very different large-scale structure as shown below.

PHASE DIAGRAMS FOR GROWTH

Fig. 2 shows phase diagrams for growth[1–6] as a function of the driving force (H or P) and effective degree of disorder (Δ or θ). Two types of transitions are evident in all phase diagrams. The first is the onset of steady growth at H_c or P_c. The second involves changes in the growth morphology. The large-scale structure at the critical force changes from self-similar to faceted as the effective degree of disorder decreases. In some cases there is an intervening regime where the interface is a self-affine fractal. We will begin by discussing growth in the limit of large disorder, and describe each transition in detail. To simplify the discussion we focus on magnetic domain growth and then comment briefly on differences in the case of fluid invasion.

When the disorder is very large, the exchange coupling can be neglected. The probability that a spin will flip becomes independent of its surroundings (ie., n). The problem reduces to site percolation since all spins with $H + h_i > 0$ will flip and all others will not. The fraction of spins which flip at H_c must equal the critical probability for normal site-

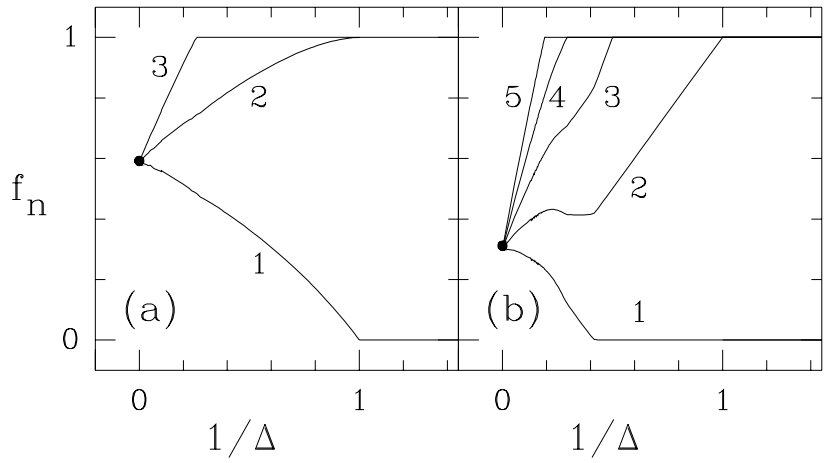

Figure 3: Probability f_n that a spin surrounded by n flipped spins will flip at H_c as a function of $1/\Delta$ on the (a) square and (b) cubic lattices. Curves are labeled by n.

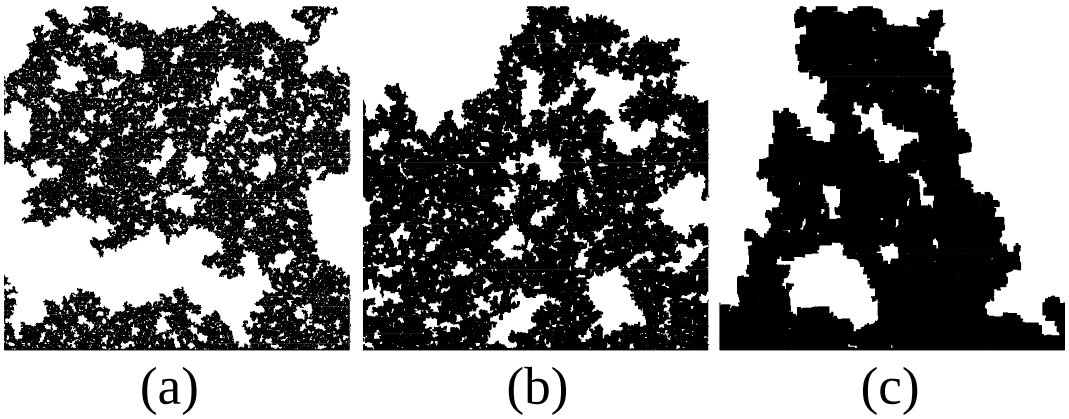

Figure 4: Invaded domains in a duct network model with $L = 512$ and $R = 10$ as θ decreases towards the critical angle $\theta_c = 48°$. The values of θ and w are: (a) $\theta = 170°$, $w = 6.8a$; (b) $\theta = 100°$, $w = 17a$; and (b) $\theta = 60°$, $w = 80a$. Equivalent changes occur in all other models as the effective degree of disorder decreases.

percolation: $p_c = 0.5927$ and 0.3117 for square and cubic lattices, respectively.[9] Figure 3 shows that this condition is satisfied. All probabilities f_n merge to p_c as $\Delta \to \infty$.

As Δ decreases, the local environment becomes increasingly important in initiating spin-flips. Spins with larger n are more and more likely to flip before other spins (Fig. 3). This leads to cooperative invasion of neighboring regions, and the pattern of flipped spins becomes smoother (Fig. 4). A measure of this change is given by the average finger width, w, calculated as the mean width of segments of adjacent flipped spins.[4] Fig. 5 shows w versus Δ for the square and cubic lattices. In all systems studied, w rises rapidly near the transition to a new type of growth morphology and then saturates at a value close to the system size.[1–8] From the behavior of the probabilities f_n and from finite-size scaling fits we have determined that $w \propto (1 - \Delta_c/\Delta)^{-\nu'}$ with $\Delta_c = 1.$, $\nu' = 1.9 \pm 0.1$ on the square lattice,[2] and $\Delta_c = 3.4$, $\nu' = 2.5 \pm 0.2$ on the cubic lattice. The exponent ν' is not universal and depends, for example, on the distribution of random fields.[2] However, one can identify universal exponents[2] relating w to the growth probabilities f_n.

Another type of universality applies to growth at all $\Delta > \Delta_C$. Despite the large change with Δ in the domains of Fig. 4, the structure at scales greater than w is always self-similar. Moreover, the fractal dimension remains equal to that for normal site percolation.[9] The box-counting method gives $D_f = 1.89 \pm 0.01$ in 2D and 2.5 ± 0.3 in

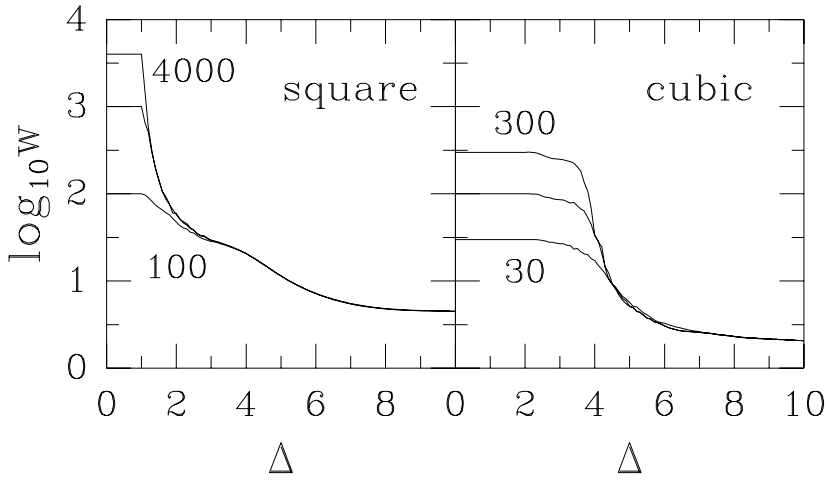

Figure 5: Variation of w with Δ on the square lattice with $L = 100$, 1000 and 4000 and the cubic lattice with $L = 30$, 100 and 300. Bends in the curves occur at points where one of the f_n becomes equal to 1 or 0.

Table 1. General scaling laws obeyed by critical exponents for invasion, and specialized forms for compact growth.[6] Here D_f and D_e are the fractal dimensions of the bulk and external hull. For compact growth D_f equals the spatial dimension and D_e=$D_f - 1$.

General	Compact Growth
$\psi = \nu(D_f + 1 - d)$	$\psi = \nu$
$\omega = \nu(D_e + 1 - d)$	$\omega = 0$
$\phi = \nu B = \nu(D_f - D_e) + 1$	$\phi = 1 + \nu$
$\tau' D_f = D_f + D_e - 1/\nu$	$\tau' d = 2d - 1 - 1/\nu$

3D, where the largest systems had $L = 4000$ and 300, respectively.[1–8]

The exponents describing the approach to the critical force can also be related to exponents for normal percolation. The correlation length, ξ, corresponds to the forward advance of the interface. As H increases to H_c, ξ, the total domain volume V, the total interface area S, and the incremental increases dV after changes in H all diverge:

$$\xi \propto (H_c - H)^{-\nu}, \quad V \propto (H_c - H)^{-\psi}, \quad S \propto (H_c - H)^{-\omega}, \quad \langle dV \rangle \propto (H_c - H)^{-\phi}. \tag{3}$$

At H_c there is a power law distribution of incremental advances[22]

$$P(dV) \propto dV^{-\tau'}. \tag{4}$$

Table 1 gives scaling laws relating these exponents to the fractal dimension and coherence length exponent ν for normal percolation. Table 2 shows that numerical values from finite-size scaling are consistent with normal percolation exponents. Note that 2D values were obtained for the disk model which includes trapping. It is known that trapping may decrease D_f in a non-universal way,[20] but our results indicate that any decrease is less than 0.05 in our model.

In Fig. 2(a) the interface becomes faceted for $\Delta < \Delta_C$. There is also a direct transition from self-similar to faceted growth in the duct network model.[8] These transitions may be understood by considering the effect of local environment on growth in the square lattice. The starting interface for our simulations was chosen to be along a line connecting nearest-neighbor spins. Unflipped spins on the interface have n=1 flipped spins and $z - 1 = 3$ unflipped spins as neighbors. The initial value of the external field in an infinite system is $H_0 = 2 - \Delta$, the lowest value at which a spin with $n = 1$ will flip. Once the first spin above the original flat interface flips, two of its neighbors have

Table 2. Critical exponents from finite-size scaling fits for wetting and non-wetting invasion of the 2D random disk model and for domain wall motion at intermediate and large disorder on the cubic lattice. Error bars in the last significant digit are indicated in parentheses. Within these uncertainties, all exponents are consistent with the scaling laws of Table 1. Within our accuracy, exponents for non-wetting invasion and domain growth at large disorder equal those for ordinary percolation.[9,22] The exponents for self-affine growth are also universal.

	$\theta = 25°$	$\theta = 179°$	2D	$\Delta = 3$	$\Delta = 6$	3D
	$P_c = .4935(5)$	$P_c = 5.62(2)$	Perc.	$H_c = 1.480(1)$	$H_c = 1.011(1)$	Perc.
D_f	2	1.88(4)	1.89...	3	2.5(1)	2.5(1)
D_e	1	1.32(2)	1.33...	2	2.5(1)	2.5(1)
α	0.81(4)			0.67(3)		
ν	1.30(5)	1.32(7)	1.33...	0.8(1)	0.9(1)	0.9(1)
τ'	1.125(25)	1.30(5)	1.31...	1.3(1)	1.6(1)	1.6(1)

equal numbers ($z/2 = 2$) of up and down spins as neighbors. For $\Delta < 1$ these spins will also flip since the maximum field required to flip a spin with $n = 2$ is $H_2^* = \Delta < H_0$. This changes the environment of two further spins to $n = 2$, and the process continues until all spins on the initial interface have flipped. Each row of spins then flips in turn until the interface reaches the top of the system. As a consequence, $H_c = H_0 = 2 - \Delta$ for $\Delta \leq \Delta_C$ and all spins in the system are flipped. In Fig. 3 the value of f_1 goes to 0 at Δ_C and $f_2 \to 1$.

The key feature in the above argument is that there is a gap between the highest force needed to flip one spin configuration and the lowest force needed to flip spins with one fewer flipped neighbor. In such cases there is no critical divergence in the invaded area as H increases to H_c. Instead, the interface is confined to a given facet over the range of forces in the gap between H_2^* and H_c. Then there is a sudden onset of growth at H_c. The moving state may exhibit critical phenomena as H is *decreased* to H_c because the fraction of sites which can flip with fewer neighbors will vanish as H decreases. The typical length scale between such sites may act like a mean-field coherence length.

Self-affine growth was only found for magnetic domain growth in 3D and highly disordered random disk models in 2D. Random disk models with small variations in throat width exhibited a direct transition to faceted growth like that in Fig. 2(a). As in the case of self-similar growth, the self-affine regime shows universal large-scale structure and critical exponents. The critical exponents satisfy the scaling relations of Table 1 and values determined from finite-size scaling[3,6] are quoted in Table 2. The calculated roughness exponent is 0.81 ± 0.04 for the disk model[5] (Fig. 6) and 0.67 ± 0.03 for the 3D Ising model.[3] The latter value is consistent with the prediction[23] of scaling arguments: $\alpha = 2/3$. The result for the random disk model is not yet fully understood, but agrees well with experimental values for invasion of glass bead packs by a wetting fluid.[17–19] We discuss the comparison between theory and experiment further in the following section.

LARGE-SCALE STRUCTURE FOR H $\neq$ H$_c$

In the preceding section we discussed the structure of pinned domains at H_c. Self-similar, self-affine or faceted structures were found depending upon the degree of disorder (Fig. 2). For $H < H_c$ the interface is pinned, but it advances a finite distance of order ξ in response to increases in H. The value of ξ diverges as $H \to H_c$ in the self-similar and self-affine growth regimes. On length scales smaller than ξ the interface exhibits the scaling behavior found at the critical force. At larger length scales the structure reflects

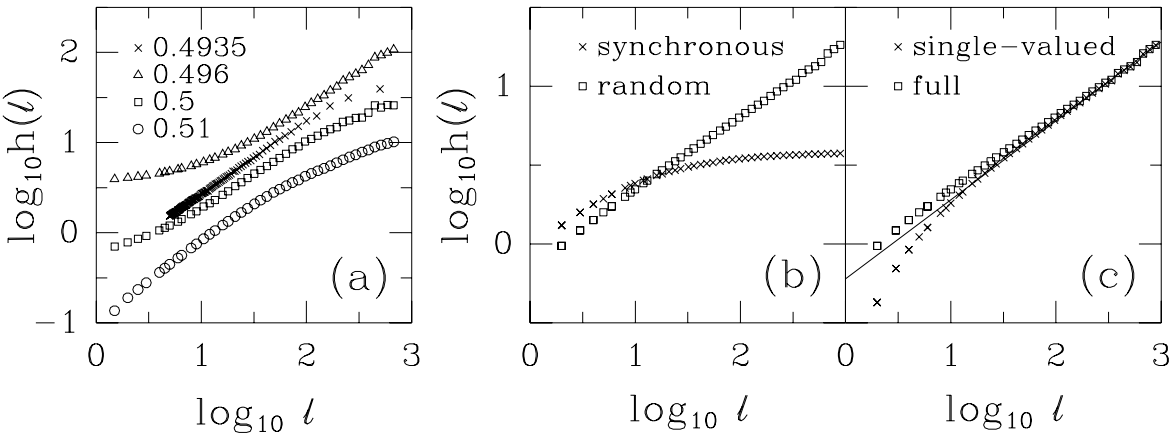

Figure 6: Fluctuation in the interface height $h(\ell)$ as a function of interval width ℓ for (a) fluid invasion of the disk model at $\theta = 25°$ and (b,c) domain growth in 2D for $\Delta = 6$ and $H = 4$. Results for the indicated pressures are compared in (a). Panel (b) compares results for synchronous and random growth algorithms and (c) compares results for the full interface and a single-valued interface consisting of the highest point at each position.

that of the starting interface. This was completely flat in most of our simulations.

Figure 6 shows that the same type of crossover occurs for forces greater than the critical force. Each panel shows the scaling of the rms width of the interface h over intervals of width ℓ. Results were typically averaged over at least ten different configurations of disks or random fields and at several different times. For a self-affine curve $h \propto \ell^{\alpha}$ where α is the roughness exponent.[10]

Panel (a) shows the scaling for fluid invasion at and above $P_c = 0.4935\gamma/a$ for $\theta = 25°$. Crosses indicate results for static interfaces obtained at the highest pressure before the interface reached the top of the system. They fall on a reasonably straight line with slope $\alpha = 0.81$. Other symbols depict results at successively higher P. Note that all exhibit roughly the same slope at intermediate scales before rounding over to a slope of about 0.5 at large scales. The crossover occurs at a dynamic coherence length which decreases as P increases. Preliminary results[26] indicate that it scales with the same exponent ν that is found below H_c (Table 2).

For P close to P_c moving interfaces may actually be rougher than static interfaces, especially at small ℓ. This reflects the influence of overhangs which develop on the growing interface. The value of h has little to do with ℓ if the surface is not a single-valued function of position along the bottom of the system. Instead h reflects the typical vertical distance between the highest and lowest points above a single position, and the frequency of overhangs. Overhangs are an essential feature of wetting invasion. The disks impede growth more in some areas than others. However, even areas that are impassable do not pin the entire interface. The interface is free to surround the bad spots and either leave small trapped regions behind or invade them from an easier direction. Overhangs form in the process of surrounding such regions, and are more prevalent in snapshots of slowly moving interfaces than in static ones. At still higher pressures the role of unfavorable regions is suppressed and there are few overhangs.

Experiments on fluid invasion have revealed similar changes in the scaling behavior with pressure.[17–19] At low velocities there is self-affine scaling with α near 0.8. At higher velocities a crossover to a lower α is observed.[18] As in Fig. 6(a) the interface appears to be self-affine with α near 0.5 at the largest scales. However, neither our simulations nor the experiments have gone to large enough scales to confirm that 0.5 is the asymptotic value of the roughness exponent. There has also been some variation in the reported

values of α at small scales.[17–19] To address these issues we have studied several models of 2D magnetic domain growth.

The structure of 2D magnetic domains at H_c is either faceted or self-similar.[1,2] As in fluid invasion, this structure persists at small length scales for $H > H_c$. New scaling behavior appears at large scales. The correlation length where the crossover occurs decreases as H increases. Figure 6(b) shows results for the self-similar regime with $\Delta = 6$, $L = 8000$ and $H = 4$. Since H is much larger than $H_c = 2.4$, the crossover occurs at $\ell \approx 10$ and the large scale behavior is revealed. When all unstable spins are flipped synchronously, the large scale structure is flat. When they are chosen randomly, $\alpha = 1/2$. These results are exactly what would be obtained in the absence of disorder where the random model becomes identical to the Eden model.[21] Thus there seems to be a common trend in the scaling of growing interfaces. They scale as if they were at the critical point up to a length $\xi \propto (f - f_c)^{-\nu}$, where f is either P or H. At larger scales, the interface behaves as if there was no disorder: Synchronous update algorithms produce flat interfaces and Eden-like algorithms produce self-affine interfaces with $\alpha = 1/2$ in 2D.

One may construct a single-valued interface from the actual interface by taking the highest value at each point. This will not change the large-scale structure of the interface if it is self-affine. However, as shown in Fig. 6(c), the behavior at small scales may be very different. The difference becomes most pronounced as H decreases towards H_c where overhangs produce a plateau in $h(\ell)$ at small ℓ for the real interface (Fig. 6(a)). The structure is self-similar at these scales and it is wrong to identify a slope in this regime with a roughness exponent. The safest way to ensure that this region of the data is not included in a fit for α is to compare the results for h with and without overhangs and exclude regions where the results differ.[26]

Overhangs may explain the difference between reported results for the roughness exponent in fluid invasion experiments. Rubio et al.[17] analyzed the full interface and found $\alpha = 0.73 \pm 0.03$, while Horvath et al.[18] analyzed the single-valued interface and found a larger value $\alpha = 0.81$. Overhangs would tend to make the former value smaller than the actual value, and the latter value larger. Analysis of both interfaces would provide an estimate of one source of systematic error. There may also be a difference in the importance of overhangs in the two experiments since they used different fluids. We find that the size and frequency of overhangs depend on θ within our model.

The observation of interfaces with $\alpha > 0.5$ was unexpected and sparked substantial interest. Most growth models map into the continuum growth equation of Kardar, Parisi and Zhang.[24] This yields $\alpha = 0.5$ in 2D and $\alpha < 0.5$ in 3D for uncorrelated noise. Larger values of α can only be produced by assuming power-law correlated noise.[25] It is not clear what sort of physical mechanism would lead to annealed power-law noise in fluid invasion. However, the power-law distribution of growths at f_c might play an analogous role.[5] The crossover to a smaller value of α at large f would then be associated with a cutoff in the distribution of growths at ξ^{D_f} and in the corresponding effective noise. A detailed relation between the disorder induced distribution of growths and the effective noise has yet to be established.

Two other explanations for the anomalously large value of α have been proposed. The most recent[28,29] are based on directed percolation models and give values of α which are slightly smaller than experiment: $\alpha \approx 2/3$. A previous calculation included quenched disorder in a continuum model of domain growth, where the interface was forced to be single-valued.[27] At large scales α approached $1/2$, but there was an apparent value of $\alpha = 0.75$ over a range of ℓ. While this result is suggestive, it is not likely to be relevant to the experiments. The calculation was done in the self-similar regime of the phase diagram where the single-valued approximation is invalid. In a more complete calculation the domain structure at small scales would be consistent with percolation. There is no

evidence of such structure in the experiments. Moreover, the region where $\alpha = 0.75$ would coincide with the region where overhangs affect the scaling of $h(\ell)$. Rubio et al.'s analysis included overhangs and would yield a plateau in this regime.[17]

SUMMARY AND CONCLUSIONS

We have illustrated the rich variety of behavior which is found when quenched disorder influences growth. At small driving forces growth is blocked by the disorder. The large-scale structure of the interface reflects the initial conditions. At large driving forces quenched disorder is unimportant. The large-scale structure is consistent with models with annealed disorder. A new large-scale structure occurs at the critical force where motion starts. For f near f_c this structure persists up to a correlation length ξ which diverges at f_c.

When the degree of disorder is large the growing domain has the form of a percolation cluster at f_c. In the extreme limit each spin or interface segment acts independently, as assumed in previous percolation models.[10,11,20] As the degree of disorder decreases, larger clusters of spins act coherently. The domains have a characteristic finger width which diverges at a transition to self-affine or faceted growth.

The transition to self-affine growth is analogous to the onset of magnetic order at an equilibrium phase transition. One can define a surface-normal correlation function: $S(l) = \langle \hat{n}(l'+l) \cdot \hat{n}(l') \rangle$, where l is the arc length along the interface and $\hat{n}$ the local surface normal. In the self-affine regime the long-distance limit of this correlation function is a constant, $S(\infty)$. The value of $S(\infty)$ rises continuously from zero at the critical transition and becomes unity in the faceted regime.[7] One may also define an effective surface tension which becomes non-zero in the self-affine regime.[5,7] Recent work[2] shows that the magnetic domain model is equivalent to a continuous set of generalized bootstrap percolation models.[30] It may be possible to obtain analytic results using this analogy.

The critical behavior which occurs as f increases to f_c is fairly well understood. Scaling relations have been derived and checked in simulations.[3,6] Studies of the behavior above f_c are in progress. The exponent ν appears to be the same on both sides of f_c. Other exponents, such as the one relating the velocity to $f - f_c$, have not yet been determined.

ACKNOWLEDGEMENTS

Support from the National Science Foundation through Grant DMR-9110004 and the Donors of the Petroleum Research Foundation, administered by the American Chemical Society is gratefully acknowledged. M.O.R. also thanks the members of the Theoretical Physics Institute at the University of Minnesota for their hospitality during the period when this work was completed.

NOTES

*Permanent address: Institute of Physics, Polish Academy of Sciences, 02-668 Warsaw, Poland.
†Current address: Physique de la Matière Condensée, College de France, 11, Place Marcelin-Berthelot, 75231 Paris Cedex 05, France.
‡Permanent address: Departamento de Física, Pontifícia Universidade Católica do Rio de Janeiro, CEP 22453, Rio de Janeiro, Brazil.
**Current address: National Institute of Standards and Technology, 226/B348, Gaithersburg, MD 20899.

REFERENCES

1. H. Ji and Mark O. Robbins, Phys. Rev. A**44**, 2538 (1991).
2. B. Koiller, H. Ji and M. O. Robbins, submitted to Phys. Rev. B.
3. H. Ji and Mark O. Robbins, to be published.
4. M. Cieplak and M. O. Robbins, Phys. Rev. Lett. **60**, 2042 (1988); Phys. Rev. **B41**, 11508 (1990).
5. N. Martys, M. Cieplak, and M. O. Robbins, Phys. Rev. Lett. **66**, 1058 (1991).
6. N. Martys, M. O. Robbins and M. Cieplak, Phys. Rev. B**44**, 12294 (1991).
7. N. Martys, PhD. thesis, (1990); N. Martys, M. O. Robbins and M. Cieplak, in *Scaling in Disordered Materials: Fractal Structure and Dynamics*, edited by J. P. Stokes, M. O. Robbins and T. A. Witten (Materials Research Society, Pittsburgh, 1990), p. 67.
8. B. Koiller, H. Ji and M. O. Robbins, Phys. Rev. B, in press.
9. D. Stauffer, *Introduction to Percolation Theory* (Taylor and Francis, London, 1985).
10. J. Feder, *Fractals* (Plenum Press, New York, 1988).
11. R. Lenormand and S. Bories, C. R. Acad. Sci. Ser. **B291**, 279 (1980). R. Chandler, J. Koplik, K. Lerman and J. F. Willemsen, J. Fluid Mech. **119**, 249 (1982).
12. M. M. Dias and A. C. Payatakes, J. Fluid Mech. 164, 305 (1986).
13. R. Lenormand, J. Phys.: Condens. Matter **2**, SA79 (1990). R. Lenormand and C. Zarcone, Phys. Rev. Lett. 54, 2226 (1985).
14. J. P. Stokes, D. A. Weitz, J. P. Gollub, A. Dougherty, M. O. Robbins, P. M. Chaikin, and H. M. Lindsay, Phys. Rev. Lett. **57**, 1718 (1986).
15. A. P. Kushnick, J. P. Stokes and M. O. Robbins, *Fractal Aspects of Materials: Disordered Systems*, (Materials Research Society, Pittsburgh, 1988) Ed. by D. A. Weitz, L. M. Sander and B. B. Mandelbrot, p. 87, and to be published.
16. J. P. Stokes, A. P. Kushnick and M. O. Robbins, Phys. Rev. Lett. **60**, 1386 (1988).
17. M. A. Rubio, C. Edwards, A. Dougherty and J. P. Gollub, Phys. Rev. Lett. **63**, 1685 (1989); *ibid.* **65**, 1339 (1990).
18. V. K. Horváth, F. Family, and T. Vicsek, Phys. Rev. Lett. **65**, 1388 (1990); J. Phys. A**24**, L25 (1991).
19. P. Z. Wong, private communication.
20. D. Wilkenson and J. F. Willemsen, J. Phys. A**16**, 3365 (1983).
21. See for example, T. Vicsek, *Fractal Growth Phenomena* (World Scientific, Singapore, 1989).
22. The exponent τ' is related to, but different from, the exponent τ describing the cluster distribution in ordinary percolation.
23. G. Grinstein and S. Ma, Phys. Rev. B**28**, 2588 (1983).
24. M. Kardar, G. Parisi, and Y. Zhang, Phys. Rev. Lett. **64**, 543 (1990).
25. E. Medina, T. Hwa, M. Kardar and Y.-C. Zhang, Phys. Rev. **A39**, 3053 (1989). J. Amar and F. Family, J. Phys. A**24**, L79 (1991).
26. B. Koiller, N. Martys and M. O. Robbins, to be published.
27. D. A. Kessler, H. Levine and Y. Tu, Phys. Rev. A**43**, 4551 (1991).
28. L. H. Tang and H. Leschhorn, to be published.
29. A.-L. Barabási, S. V. Buldyrev, F. Caserta, S. Havlin, H. E. Stanley and T. Vicsek, to be published.
30. J. Chalupa, P. L. Leath and G. R. Reich, J. Phys. C. **12**, L31 (1981): P. M. Kogut and P. L. Leath, J. Phys. C **14**, 3187 (1981); J. Adler and J. Aharony, J. Phys. A **21**, 1387 (1988).